Select type of manuscript: Research Paper

The Formation Transformation of the UUVs Based on the Leader-Follower Strategy and the Binary-Tree Structure

Junxi Zhang [*], Bin Xin[,†], Qing Wang[**] and Yun Qu[**]**

[*] School of Automation, Beijing Institute of Technology, Beijing, China
[**] State Key Laboratory of Intelligent Control and Decision of Complex Systems, Beijing Institute of Technology, Beijing, China
E-mail: brucebin@bit.edu.cn

This paper addresses the approaches for the formation transformation of the Unmanned Underwater Vehicles (UUVs), which only rely on sensor measurement. Due to the limited measuring range, the leader-follower strategy and the binary-tree structure are employed to design the desired formation and the switching process. In order to achieve the desired formation, the controller for each follower UUV is designed with the integral sliding mode method, which makes the follower surge velocity and heading angle achieve consistent with the leader UUV. The simulation results demonstrate the formation transformation can be achieved, and the approaches adopted in the paper are effective.

Keywords: Unmanned Underwater Vehicles, Formation Transformation, Leader-Follower, Binary-Tree and Integral sliding mode control

1. Introduction

With the improvement of the task complexity, it is more and more difficult for a single agent to complete the tasks. Multi-agent cooperation, however, can increase the redundancy and robustness of the system and improve the efficiency of task execution[1]. In this case, the formation control attracted people's attention and became an important study field of multi-agent system, which requires that the agents can form the desired formation.

The common strategies for formation control include leader-follower strategy[2,3,4], behavior based strategy, artificial potential field strategy[5,6] and virtual structure strategy[7]. Among them, the leader-follower strategy is very effective to realize the distributed control. The common methods for tracking control include sliding mode control[3,8,14], backstepping control[9,10], event-triggered strategy[15] and so on. Shikun Pang et al[2] designed an inversion controller by using Lyapunov function, so that the follower's trajectory can converge to the reference path in a short time and the desired formation can be obtained. However, the control law is relatively complex and may be difficult to implement in engineering. Zheping Yan et al[8] applied integral sliding mode control to the trajectory tracking of the underactuated UUV with parameter perturbation. Juan Li et al[3] proposed a robust sliding mode formation control method based on leader-follower strategy and designed integral sliding mode surface for the velocity error of the follower. However, the author only illustrated the formation of three UUVs. As for the formation of more UUVs, the vibration of the leaders will be transmitted to the follower, which may aggravate the vibration of the follower. Based on the above literatures, this paper realizes the formation of 5 UUVs based on integral sliding mode control and PID control. The follower UUV can track the leader UUV with this method, and the appropriate parameters can be designed to help reduce the vibration of the follower UUV.

The above references mainly studied the formation generation and maintenance. In practice, different formations are needed to adapt to different environments and finish different tasks, so the study of formation transformation is significant. According to the literature we investigated, most of the related researches are focused on the UAV, and there are less researches on the switching formation of UUV. Daifeng Zhang et al[11] proposed a novel switching formation method for quadrotor UAV based on binary-tree, which can realize the transformation between the herringbone-shape and the complete binary-tree shape topology of 7 UAVs. With the use of binary-tree, this method simplifies the rules of formation transformation and saves computing costs. However, this conference did not consider the complicated aerodynamics of UAV，and the switching process relied on the information of communication. However, underwater communication is seriously limited, unable to transmit a large amount of information. Therefore, sensors are necessary in underwater environment, which motivates our research for UUV formation control with measurement constraints. Therefore, the paper introduced the hydrodynamic model of UUV and binary-tree topology is adopted to formation transformation of UUVs. Furthermore, herringbone-shape formation is set as the standard formation.

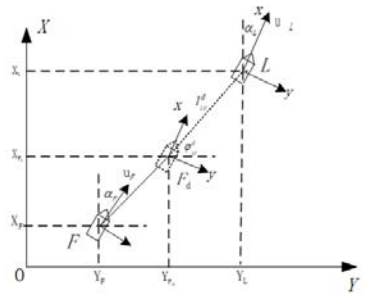

Fig. 1 The leader-follower model

The main contributions in this paper are as follows: i)The detailed approaches are given to achieve formation transformation of 5 UUVs, which only rely on sensor measurement. The transformation among herringbone-shape and line-shape and spear-shape are considered in this paper. ii) This paper points out the problems of using the sliding mode tracking controller during the switching process, and puts forward some improved methods.

The contents of this paper are as follows: The model of the UUV, the measurement limitation and the binary-tree topology are described in Section 2. In Section 3, the control system of the follower UUV is introduced. The detailed formation transformation rules are introduced in Section 4. In Section 5, the simulation results are shown, and the paper is summarized in Section 6.

2. Problem Description

The model of the UUV and the binary-tree topology of the formation are introduced in this section. The section also includes the description of the limited measuring range.

2.1. The model of the UUV

Figure. 1. shows the leader-follower model of the UUVs, which is based on the model in reference [2]. $V=(u,v,r)^T$,where (u,v) are the surge and sway velocities and r is the angular velocity of the UUV in the body coordinate system. $\mu=(X,Y,\alpha)^T$,where (X,Y) is the coordinate of the UUV in the Cartesian coordinate system, and the heading angle α is defined as the angle between the UUV orientation and the positive X axis of the coordinate system.

the kinematic model of the UUV is

$$\begin{aligned}\dot{X}&=ucos\alpha-vsin\alpha\\ \dot{Y}&=usin\alpha+vcos\alpha.\\ \dot{\alpha}&=r\end{aligned}\tag{1}$$

The transformation matrix between the UUV body coordinate system and the cartesian coordinate system is defined as

$$R(\alpha)=\begin{bmatrix}cos\alpha & -sin\alpha & 0\\ sin\alpha & cos\alpha & 0\\ 0 & 0 & 1\end{bmatrix}.\tag{2}$$

The hydrodynamic model of UUV[12] is

$$\begin{cases}\dot{\mu}=R(\alpha)V\\ M\dot{V}=\tau-C(V)V-D(V)V\end{cases}\tag{3}$$

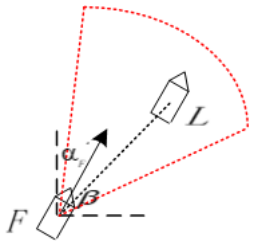

Fig. 2. The measuring range of the laser sensor

where $C(V)$ is a skew-symmetric matrix of Coriolis, and $D(V)$ is a nonlinear damping matrix. M is the system inertia matrix. The definition and parameter setting of $C(V), D(V)$ and M can be referred to [12]. The vector $\tau=(\tau_u,\tau_v,\tau_r)^T$ is the control force and the moment. Because the UUV considered is underactuated, $\tau_v=0$.

2.2. The Measurement Limitation

The UUV considered has a laser sensor at the head. The follower UUV confirms its leader UUV and the relative position with the leader by using the measurement information. The measurement range of the laser sensor is limited. We set the measurement angle range of UUV to $\pm\vartheta$ and the farthest measurement distance to S_{max}, which are shown in **Fig. 2**.

2.3. The Topology of the Formation

In this paper, the directed graph $D=(P,E,A)$ is used to represent the formation topology. $P=\{p_1,p_2,\ldots,p_N\}$ is the set of all UUVs and E is the set of all edges. Each edge is oriented from the leader to its follower. A is the adjacency matrix of the topology.

According to the leader-follower strategy and the constraints of the measurement, the formation that the UUVs can organize is designed as a tree structure with the main leader UUV as the root node.

The state of the follower UUV will not be fed back to its leader, so it is necessary to design the specific rules for each UUV to realize the formation transformation. To simplify the rules, the binary-tree structure is employed to design the formation topology and the switching process. Each node in the binary-tree can have at most two children. In other words, each leader in the formation has at most two followers. The subtree represented by the child node is called the left subtree or the right subtree[11], which is determined by the relative position of the follower to its leader. **Fig. 3** shows the herringbone-shape, the spear-shape and the line-shape formation of 5 UUVs designing by binary-tree.

3. The control System of the Follower UUV

In order to enable the follower UUV to track its leader, the control system of the follower UUV is designed as **Fig. 4**. The kinematic controller is

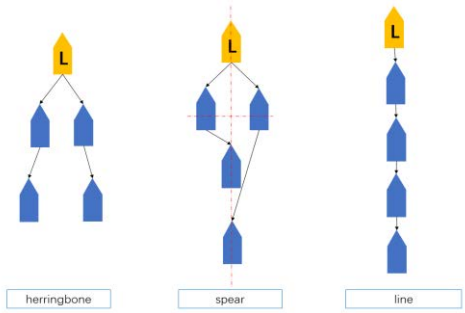

Fig. 3 The tree formations of the herringbone-shape, the spear-shape and the line-shape

designed with the integral sliding mode control and the leader-follower strategy. The PID method is applied in the dynamic controller. F_d is the desired point of the follower UUV.

The kinematic controller calculates the errors of μ and V and adjusts the control laws of heading angle α_F^d and surge velocity u_F^d. u_F^d and α_F^d are the reference inputs of PID controller. The outputs of PID controller adjust the control force and the moment $\tau = (\tau_u, \tau_v, \tau_r)^T$ of UUV, so that UUV can update its states. Then the states feed back to the kinematic controller and PID dynamic controller.

3.1. The Leader-Follower model

The leader-follower model applied refers to the formation model in reference[2], and the calculation is simplify on the basis of it. The sketch map of the leader-follower model is shown in **Fig. 1**. The distance between the leader and the follower is denoted by l_{LF}, and the relative angle of sight is denoted by φ_{LF}. The desired values of them are l_{LF}^d and φ_{LF}^d. $\mu_{F_d} = \left(X_{F_d}, Y_{F_d}, \alpha_{F_d}\right)^T$ can be calculated by

$$\begin{cases} Y_{F_d} = Y_L - l_{LF}^d cos\varphi_{LF}^d \\ X_{F_d} = X_L - l_{LF}^d sin\varphi_{LF}^d \\ \alpha_{F_d} = \alpha_L \end{cases}. \tag{4}$$

$V_{F_d} = \left(u_{F_d}, v_{F_d}, r_{F_d}\right)^T = V_L$, so V_L will replace V_{F_d} for calculation in the following.

The position deviations between the follower UUV and the leader UUV in the leader's body coordinate system are denoted by $E_1 = (e_x, e_y)^T$, in which

$$\begin{cases} e_x = (Y_{F_d} - Y_F)sin\alpha_L + (X_{F_d} - X_F)cos\alpha_L \\ e_y = (Y_{F_d} - Y_F)cos\alpha_L - (X_{F_d} - X_F)sin\alpha_L \end{cases}. \tag{5}$$

The deviations of the heading angle between the leader UUV and the follower UUV is defined as

$$e_\alpha = \alpha_L - \alpha_F \ . \tag{6}$$

3.2. The Design of the Kinematic Controller

With (2), (7) and (8) it can be obtained that

$$\begin{cases} \dot{e_x} = u_L - u_F cose_\alpha - v_F sine_\alpha + e_y\dot{\alpha_L} \\ \dot{e_y} = v_L + u_F sine_\alpha - v_F cose_\alpha - e_x\dot{\alpha_L} \\ \dot{e_\alpha} = \dot{\alpha_L} - \dot{\alpha_F} \end{cases}. \tag{7}$$

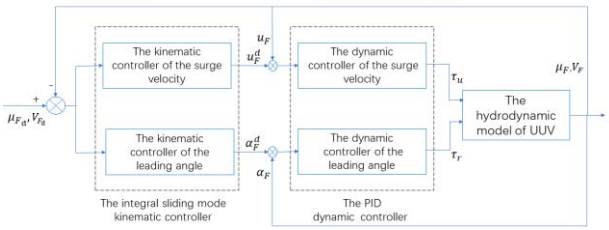

Fig. 4 Control system of the follower UUV

The rotation matrix between the body coordinate systems of the leader and the follower is defined as

$$R_1(\alpha) = \begin{bmatrix} cose_\alpha & -sine_\alpha \\ sine_\alpha & cose_\alpha \end{bmatrix}. \tag{8}$$

The position deviations between the follower UUV and the leader UUV in the follower's body coordinate system is denoted by $E_2 = (\varepsilon_1, \varepsilon_2)^T$, and

$$E_2 = R_1(\alpha) \times E_1. \tag{9}$$

By deriving ε_1 it can be obtained that

$$\dot{\varepsilon_1} = -\varepsilon_2\dot{e_\alpha} + u_F + \rho_1 + \rho_2, \tag{10}$$

where

$$\rho_1 = -cose_\alpha\left(e_y\dot{\alpha_L} + u_L\right),$$
$$\rho_2 = sine_\alpha(v_L - e_x\dot{\alpha_L}). \tag{11}$$

An integral sliding mode controller which can eliminate the reaching process and thus improves robustness is used to get the reference surge velocity u_F^d. The first order sliding mode surface[3] is designed as

$$S = \varepsilon_1 + k_1\left(\int_0^t \varepsilon_1(\tau)d\tau + \varepsilon_1'(0)\right). \tag{12}$$

where $k_1 \in R_+$. $\varepsilon_1'(0)$ is the value of the integral term when $t = 0$. We suppose

$$\varepsilon_1'(0) = -\frac{1}{k_1}\varepsilon_1(0), \tag{13}$$

so that $S = 0$ when $t = 0$. This shows the initial state is on the sliding mode surface.

By deriving S we can get

$$\dot{S} = \dot{\varepsilon_1} + k_1\varepsilon_1. \tag{14}$$

If $\dot{S} = 0$, $S = 0$ at any time. By substituting (10) into it, the desired value of surge velocity can be calculated by

$$u_F^d = -k_1\varepsilon_1 + \varepsilon_2\dot{e_\alpha} - \rho_1 - \rho_2. \tag{15}$$

In order to ensure that the follower reaches the desired point F_d, it's necessary to make the orientation of the follower point to F_d. The angle relation between the follower and F_d is shown in **Fig. 5**. The desired value of heading angle is

$$\alpha_F^d = \alpha_L + arctan\left(\frac{e_y}{b}\right), \tag{16}$$

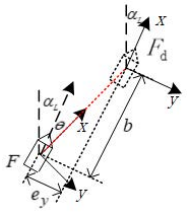

Fig. 5 The angle relation

where $b \in R_+$.

3.3. The Design of the Dynamic Controller

Two PID controllers, whose reference inputs are u_F^d, α_F^d, are designed to get the control force and the moment $\tau = (\tau_u, \tau_v, \tau_r)^T$ of UUV,

$$\begin{cases} \tau_u \propto K_{p_1}((u_F^d - u_F) + \frac{1}{T_{I_1}}\int_0^t (u_F^d - u_F)dt + T_{D_1}\frac{d(u_F^d - u_F)}{dt}) \\ \tau_v = 0 \\ \tau_r \propto K_{p_2}((\alpha_F^d - \alpha_F) + \frac{1}{T_{I_2}}\int_0^t (\alpha_F^d - \alpha_F)dt + T_{D_2}\frac{d(\alpha_F^d - \alpha_F)}{dt}) \end{cases}, \quad (17)$$

where $K_{p_1}, K_{p_2}, K_{p_1}, T_{I_1}, T_{I_2}, T_{D_1}, T_{D_2} \in R$, $T_{I_1}, T_{I_2}, T_{D_1}, T_{D_2} \neq 0$. Equation (17) shows that the outputs of PID controller adjust the values of τ. The maximum values are determined by the structure of UUV and the actuator configuration. The paper sets $|\tau_u| \leq 2.0\text{N}, |\tau_r| \leq 2.0\text{N} \cdot \text{m}$.

3.4. Stability Analysis

We define the following Lyapunov function.

$$\text{V}_{\text{Lya}} = \frac{1}{2}({\varepsilon_1}^2 + {\varepsilon_2}^2). \quad (18)$$

With the control law (16), the orientation of the follower point to F_d, so $\varepsilon_2 = 0$.

By deriving formula (18) we can get

$$\begin{aligned} \dot{V}_{Lya} &= \varepsilon_1\dot{\varepsilon_1} + \varepsilon_2\dot{\varepsilon_2} \\ &= -k_1{\varepsilon_1}^2 + 0 \leq 0. \end{aligned} \quad (19)$$

ε_1 can converge to 0.

Thanks to the wide range of applications and good performance of PID method, the stability analysis of the errors of α_F and u_F is omitted.

4. The Formation Transformation Based on the Binary-Tree

This section describes the design of the formation transformation process based on the binary-tree, and the controller introduced in Section 3 is used to adjust the relative position of the follower UUV to its leader. At the same time, the problems of using the sliding mode tracking controller during the switching process are pointed, and some corresponding improved method are put forward.

Before designing the transformation process, it is needed to confirm the left and right subtrees of the main leader UUV p_1. For the follower UUV p_i of p_1,

$$\begin{cases} \varphi_{LF}^d + \alpha_L \leq \frac{\pi}{2}, & p_i \text{ and its followers belong to the left subtree} \\ \varphi_{LF}^d + \alpha_L > \frac{\pi}{2}, & p_i \text{ and its followers belong to the right subtree} \end{cases} \quad (20)$$

The UUVs of the left and the right subtrees follow different transformation rules.

In order to simplify the rules, this paper sets the herringbone formation as the standard formation. The herringbone formation can be directly converted into the line and the spear. The conversion between the line formation and the spear needs to be mediated by the herringbone formation.

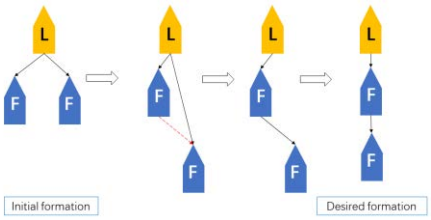

Fig. 6 Formation transformation of the 3 UUVs

4.1. The transformation process of 3 UUVs

In the process of the transformation, there are two operations needed, which are adjusting the position of the follower UUV relative to the leader and changing the leader of the follower UUV. The group of 3 UUVs is the smallest unit that can realize the above two operations. The transformation process of 3 UUVs from herringbone-shape to line-shape is shown in **Fig. 6**.

The rules summarized from **Fig. 6** are as follow.

The rules for the left-subtree node: adjust φ_{LF}^d so that $\varphi_{LF}^d + \alpha_L = \frac{\pi}{2}$ (the follower goes forward in the line-shape with the leader).

The rules for the right-subtree nodes:

- Step 1: Stay away from the leader so that it can detect both the leader and the left subtree node at the same time.
- Step 2: Take the left subtree node as the leader, then adjust φ_{LF}^d so that $\varphi_{LF}^d + \alpha_L = \frac{\pi}{2}$.

4.2. The transformation process of 5 UUVs

Based on the formation transformation rules of 3 UUVs, the formation transformation process of more UUVs is designed as follow. The UUV in the topology are layered firstly. The main leader UUV p_1 belongs to layer 0. If one UUV belongs to layer m (m>0), its leader belongs to layer m−1. In the herringbone formation in **Fig. 3**, there are two nodes in layer m (m>0). They belong to the left subtree and the right subtree respectively and are recorded as p_{left}^m and p_{right}^m. Suppose there are N_l nodes in the left subtree and N_r nodes in the right subtree of p_1, the transformation rules between the line and the herringbone formation are introduced as follow.

The rules for the left subtree nodes: go forward in the line-shape with the leader and shorten the distance with the leader.

The rules for the right subtree nodes:

- Step 1: p_{right}^1 stay away from p_1 until it can detect both p_1 and p_{left}^1 at the same time. Other nodes of the right subtree go forward in the line-shape with p_{right}^1.

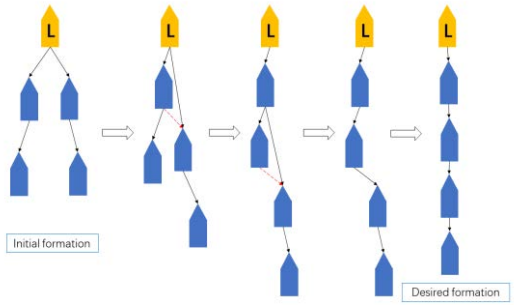

Fig. 7 Formation transformation of the 3 UUVs

- Step 2: p^1_{right} takes p^1_{left} as its leader, then stay away from p^1_{left} until it can detect both p^1_{left} and p^2_{left} at the same time.
- Step 3: p^1_{right} takes p^2_{left} as its leader, then go forward in the line-shape. Finally, p^1_{right} takes $p^{N_l}_{left}$ as its leader.

The transformation process of 5 UUVs from the herringbone to the line formation resorting to the above rules is shown in **Fig. 7**. The rules opposite to the above can realize the transformation from the line formation to the herringbone, which is deferent from reference [11]. p^1_{left} keep moving forward and finally takes p_1 as the leader. Other UUVs return to their positions in the herringbone formation.

Conversion between the herringbone formation and the spear formation does not require the UUVs change their leaders. Only the positions of the last layer nodes relative to first layer nodes need to be adjusted. The desired spear formation is shown in **Fig. 3**.

4.3. The improvement of the rules

Because of the application of the sliding mode method in the follower UUV's kinematic controller, the big change of the reference input will lead to the output oscillation and even the output divergence. Therefore, some improvement of the rules are proposed to help reduce the output oscillation.

- When the follower UUV moves forward/ backward for a long distance relative to its leader, the desired value of the relative distance l^d_{LF} increases/decreases linearly, instead of the large step input to the kinematic controller.
- Considering the cascade structure of the UUVs, the vibration of the leader UUV's stage will affect the follower. So it is necessary to wait for a period of time before executing the next rule in the transformation process, so that the follower has enough time to reach the stable state.

5. Simulation Results

Some parameters of the desired formation of 5 UUVs in the simulation are given as **Table 1**.

Table. 1 Parameter setting.

	herringbone		***line***		***cross***	
	l^d_{LF}	l^d_{LF}	l^d_{LF}	φ^d_{LF}	l^d_{LF}	φ^d_{LF}
p^1_{left}	$5.0m$	$\pi/5$	$2.0m$	$\pi/2 - \alpha_L$	$5.0m$	$\pi/5$
p^1_{right}	$5.0m$	$\pi/3$	$2.0m$	$\pi/2 - \alpha_L$	$5.0m$	$\pi/3$
p^2_{left}	$3.0m$	$\pi/5$	$3.0m$	$\pi/2 - \alpha_L$	$3.0m$	$\pi/3$
p^2_{right}	$3.0m$	$\pi/3$	$2.0m$	$\pi/2 - \alpha_L$	$7.0m$	$\pi/5$

The leader's preset trajectory is a line with a slope of 1. The initial values of V and μ of the leader and the followers are given as follow: $V_L = V^l_F = V^r_F = (0,0,0)^T$; $\mu_L = (40,0,0)^T$, $\mu^1_{left} = (35,-3,0)^T$, $\mu^1_{right} = (37,-5,0)^T$, $\mu^2_{left} = (30,-6,0)^T$, $\mu^2_{right} = (34,-10,0)^T$.

5.1. The Formation of the Herringbone

Figure. 8 shows the trajectories of 5 UUVs when forming the herringbone. There is no intersection among the tracks, which means there is no collision among the UUVs. No UUV dropping out also indicates that the follower UUV and its leader meet the measurement constraints.

Figure. 9 show the surge velocity and leading angle curves of 5 UUVs. It can be seen from the figure that

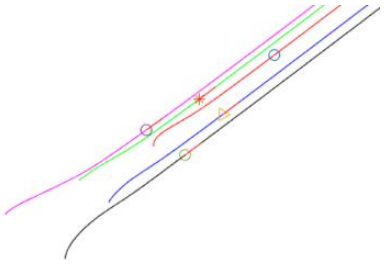

Fig. 8 The Herringbone formation of 5 UUVS

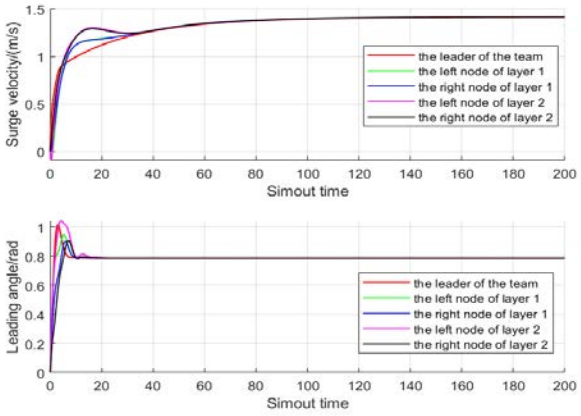

Fig. 9 Surge velocity and leading angle curves of the 5 UUVs

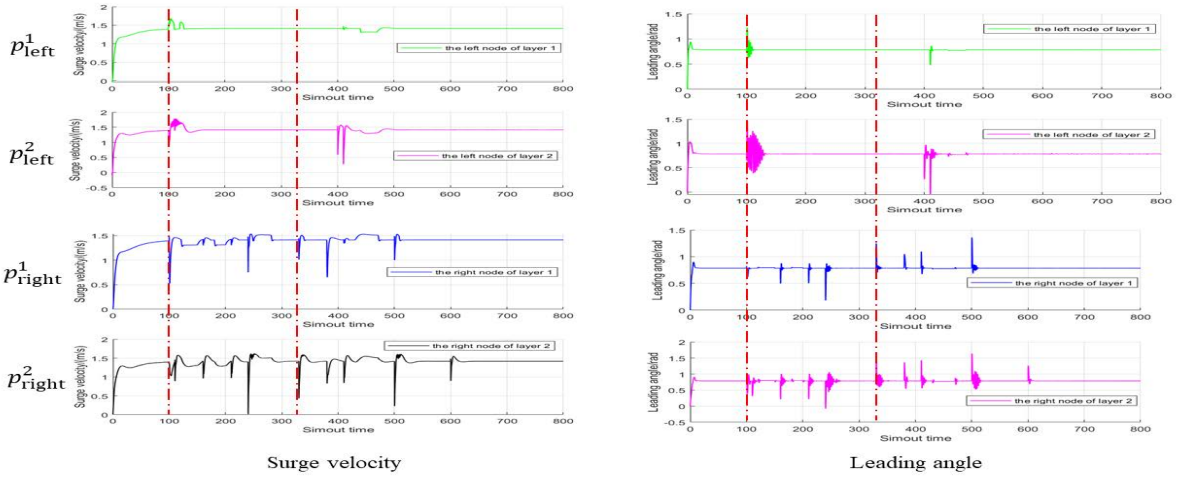

Fig. 11 The surge velocity and the leading angle curves of 4 follower UUVs

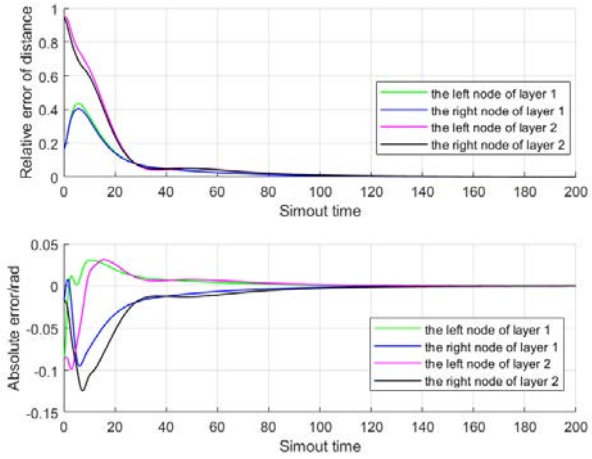

Fig. 10 The formation error of the follower UUVs

the velocities and the forward directions of the 5 UUVs can be consistent finally.

Figure. 10 shows the relative error of the relative distance l_{LF} and the absolute error of the relative angle of sight φ_{LF}. The figure proves the follower UUVs can reach the desire point in the formation.

5.2. The Transformation process between the Herringbone and the Line Formation

According to the formation transformation rules designed in Section 4, the simulation is carried out and the results are shown as follow.

Figure. 11 show the surge velocity and the leading angle of 4 follower UUVs. The first red dotted line indicates the starting time of the transformation process from the herringbone to the line, and the second indicates the starting time of the transformation process from the line to the herringbone. The oscillation of p^1_{left} and p^1_{right} will make p^2_{left} and p^2_{right} produce more violent oscillation, which is the problem of applying the sliding mode method. p^1_{right} and p^2_{right} employ the improved method introduced in Section 4 while p^1_{left} and p^2_{left} do not apply it. It can be seen from the results that the oscillation

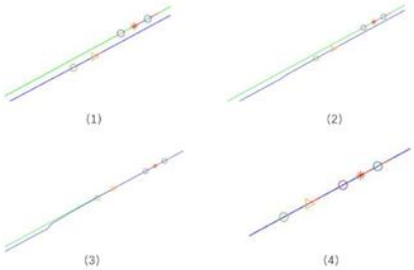

Fig. 12 the formation transformation process from the herringbone to the line. (1) The left subtree nodes keep straight ahead with the main leader of the team, and the right subtree nodes close to the main leader's track. p^1_{right} changes its leader to p^1_{left}. (2) p^1_{right} changes its leader to p^2_{left}. (3) p^1_{right} and p^2_{right} go straight ahead with p^2_{left}. (4) Adjust the relative distance between nodes to achieve the desired straight line formation

frequency and the amplitude of the heading angle of p^2_{right} is smaller than that of p^2_{left}, which shows that the improved method is effective.

The mutation of the values shown in **Fig. 11** corresponds to the four processes shown in **Fig. 12**. The velocities and the leading angles of the 5 UUVs can be consistent finally.

In the transformation process between herringbone and cross, only the UUVs of layer 2 is needed to change the relative position with their leader. The cross formation is shown in **Fig. 13**.

Figure. 14 show the surge velocity curves and the leading angle curves of p^2_{left} and p^2_{right}.

Fig. 13 The cross formation of 5 UUVs. The purple circle is p^2_{left} and the green circle is p^2_{right}

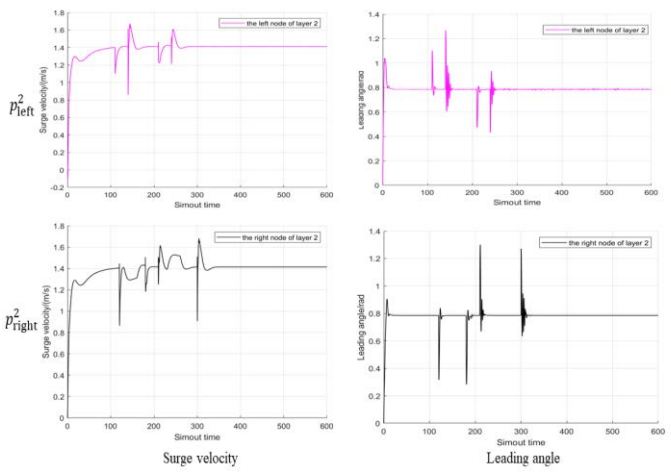

Fig. 14 the surge velocity curves and the leading angle curves of p^2_{left} and p^2_{right}

6. Conclusion

In this paper, the rules of formation transformation based on leader-follower strategy are designed for UUVs with measurement constraints. The formation controller for follower UUV is designed with integral sliding mode control and some other calculation methods. In this way, the follower can reach the desired position in the formation and move forward at the same speed and direction as the leader. The simulation results show the UUVs can achieve the formation and verify the effectiveness of the methods employed in the paper. The methods designed in this paper are applicable to a small amount of UUVs. In future work, the authors will try to expand the formation scale and design formation transformation rules in reference to the bionic mechanism (such as the movement of fish) to get the more applicable topology model.

Acknowledgements

The work was supported in part by the National Outstanding Youth Talents Support Program 61822304, the National Natural Science Foundation of China under Grant 61673058, the NSFC-Zhejiang Joint Fund for the Integration of Industrialization and Informatization under Grant U1609214, the National Key R&D Program of China (2018YFB1308000), and sponsored by Peng Cheng Laboratory, and Beijing Advanced Innovation Center for Intelligent Robots and Systems.

References:

[1] Zheping Yan, Xiangling Liu, “Research Status and Development Trend of Multi-UUV Coordinated Control Technology,” Journal of Unmanned Undersea Systems, vol. 27, pp. 226–231, Mar. 2019.

[2] Shikun Pang, Jian Wang, Hong Yi, and Xiaofeng Liang, “Formation Control of Multiple Autonomous Underwater Vehicles Based on Sensor Measuring System,” Journal of Shanghai Jiaotong University, vol. 53, pp. 549–555, May 2019.

[3] Juan Li, Tao Ma, and Jianhua Liu, “Multi-UUV coordinated formation sliding mode control based on leader,” Journal of Harbin Engineering University, vol. 39, pp. 350–357, Feb. 2018.

[4] Zheping Yan , Yibo Liu, and Changbin Yu, “Leader-following coordination of multiple uuvs formation under two independent topologies and time-varying delays,” Journal of Central South University, vol. 24, pp. 382–393, Feb. 2017.

[5] Nair, Ranjith Ravindranathan , et al. "Multisatellite Formation Control for Remote Sensing Applications Using Artificial Potential Field and Adaptive Fuzzy Sliding Mode Control," IEEE Systems Journal, vol. 9, pp. 508-518, Feb. 2015.

[6] Yongshen, Lv , et al. "Formation control of UAVs based on artificial potential field," CA: Chinese Control And Decision Conference (CCDC) , 2018.

[7] Qin, Qi , et al. "Virtual Structure Formation Control via Sliding Mode Control and Neural Networks," CA: International Symposium on Neural Networks Springer, Cham, 2017.

[8] Zheping Yan, Xiang Li, and Yuwu Song, “Trajectory Tracking Control Method for Underactuated UUV Using Integral Sliding Mode under Parameter Perturbation,” Journal of Unmanned Undersea Systems, vol. 26, pp. 500–506, Mar. 2018.

[9] Guo, Yong , S. M. Song, and X. H. Li, "Backstepping sliding mode control for formation flying spacecraft," Aircraft engineering, vol. 90, pp. 56-64, Jan. 2018.

[10] Rout, Raja, Subudhi, and Bidyadhar, " A backstepping approach for the formation control of multiple autonomous underwater vehicles using a leader-follower strategy," Journal of Marine Engineering and Technology, vol. 15, pp. 38-46, Jan. 2016.

[11] Daifeng Zhang and Haibin Duan, " Switching topology approach for UAV formation based on binary-tree network," Journal of the Franklin Institute, vol. 356, pp. 835-859, Jan. 2019.

[12] Skjetne, Roger, T. I. Fossen, and Petar V. Kokotović. “Adaptive maneuvering, with experiments, for a model ship in a marine control laboratory,” Automatica, vol. 41, pp. 289–298, Feb. 2005.

[13] Shi-Lu Dai , Shude He , Xin Chen, and Xu Jin. “Adaptive Leader–Follower Formation Control of Nonholonomic Mobile Robots With Prescribed Transient and Steady-State Performance,” IEEE Transformation on Industrial Information, vol. 16, pp. 3662–3671, June. 2020.

[14] Xin Linjie, Wang Qinglin, Li Yuan, and She Jinhua. “Adaptive fast terminal sliding mode control for a class of uncertain systems with input nonlinearity, ” Journal of Advanced Computational Intelligence and Intelligent Informatics, vol. 21, pp. 518-526, May. 2017.

[15] Zhou Feng, Huang Zhiwu, Liu Weirong, and Li Liran. “Formation control with event-triggered strategy for multi-agent systems, ” Journal of Advanced Computational Intelligence and Intelligent Informatics, vol. 18, pp. 71-77, Jan. 2014.